Theoretical insights into photochemical ESITP process for novel DMP-HBT-py compound*

Guang Yang(杨光)[1,†], Kaifeng Chen(陈凯锋)[1], Gang Wang(王岗)[1], and Dapeng Yang(杨大鹏)[2]

[1] *Basic Teaching Department, Jiaozuo University, Jiaozuo* 454000, *China*

[2] *Collaborative Innovation Center of Light Manipulations and Applications, Shandong Normal University, Jinan* 250358, *China*

(Received 21 June 2020; revised manuscript received 15 July 2020; accepted manuscript online 28 July 2020)

We execute the density functional theory (DFT) and time-dependent density functional theory (TDDFT) approaches to make a detailed exploration about excited state luminescent properties as well as excited state intramolecular proton transfer (ESIPT) mechanism for the novel 2,6-dimethyl phenyl (DMP-HBT-py) system. Firstly, we check and confirm the formation and stabilization of hydrogen bonding interaction for DMP-HBT-py. Via optimized geometrical parameters of primary chemical bond and infrared (IR) spectra, we find O–H···N hydrogen bond of DMP-HBT-py should be strengthened in S_1 state. Insights into frontier molecular orbitals (MOs) analyses, we infer charge redistribution and charge transfer (ICT) phenomena motivate ESIPT trend. Via probing into potential energy curves (PECs) in related electronic states, we come up with the ultrafast ESIPT behavior due to low potential barrier. Furthermore, we search the reaction transition state (TS) structure, the ultrafast ESIPT behavior and mechanism of DMP-HBT-py compound can be re-confirmed. We sincerely wish this work could play roles in further developing novel applications based on DMP-HBT-py compound and in promoting efficient solid emitters in OLEDs in future.

Keywords: infrared vibrational spectra, intramolecular charge transfer, potential energy curve, excited state intramolecular proton transfer

PACS: 31.15.ee, 31.15.ae, 31.15.es **DOI:** 10.1088/1674-1056/aba9bb

1. Introduction

To the best of our knowledge, as a typical weak interaction, hydrogen bonding effects undoubtedly play momentous roles in various photochemical and photo-physical behaviors in nature.[1–10] It is immanent in liquids and crystallization of materials. What is more, hydrogen bond dominants structural stabilities of biomolecules, such as DNA and RNA.[11–15] Because of dynamical properties of hydrogen proton, hydrogen bond could also act the active sites for activating plenty of chemical and biological reactions. Accordingly, it is vital to expound various phenomena involved in hydrogen bonding dynamics. As is known to all, explorations on excited state intramolecular proton transfer (ESIPT) reaction along with pre-existing hydrogen bond have become the hotspot in photochemical and photo-biological domains.[16–30] Generally, molecules or systems with ESIPT properties could exhibit dual fluorescence peaks under specific photo-excitation. One fluorescence peak could be resulted from initial molecular structure prior to ESIPT behavior (*i.e.*, enol configuration), and the other one derives from the form after ESIPT reaction (*i.e.*, keto structure).[16–30] Via comparing with the emission peak of the former, it can be found the fluorescence of the latter one shows obvious red-shift. On account of this kind of characteristics, practical applications could be expired such as light emitting diodes, fluorescence sensors, molecular switches, cell imaging, and so forth.[31–44]

To be specific, energy gap between Franck–Condon excited state and relaxed excited state furnishes the driving force for transformation of proton. In turn, the slope of these two states resolves relative kinetics. In most cases, this kind of reaction follows reaction cycle, namely, absorption → ESIPT → fluorescence → inverted S_0-state PT. As mentioned above, in consideration of the distinction of double fluorescence peaks, the large Stokes shift could be demonstrated.[31–44] In other words, observation of a nearly mirror symmetry between absorption and fluorescence spectra illustrates the nuclear configuration of the molecule and its surrounding medium remains close to that of S_0 state over excited state lifetime,[31–44] while the effects of ESIPT on Franck–Condon factors are enough to destroy this kind of mirror symmetry.

It is well known the 2-(2-hydroxyphenyl)benzothiazole (HBT) is a typical ESIPT compound, which has been extensively investigated since its derivatives could be facilely obtained via simple chemical modifications at various coordination positions. Recently, Niu and coworkers described and reported a new 2,6-dimethyl phenyl (DMP-HBT-py),[45] which might undergo ESIPT reaction. Further, given the aggregation case, DMP-HBT-py system also presents its aggregation-induced emission (AIE) property, which might own potential as an efficient solid emitter in OLEDs. Therefore, the novel

*Project supported by the Science and Technology Research Project of Henan Province, China (Grant No. 172102210391) and the Higher Vocational School Program for Key Teachers from Department of Education of Henan Province, China (Grant No. 2019GZGG042).

†Corresponding author. E-mail: yxd5460@163.com

DMP-HBT-py compound and its derivatives might be a better ESIPT model for further embellish and explore novel applications based on them. It cannot be denied the straightforward photo-induced excitation characteristics and excited state overall perspective DMP-HBT-py is necessary for further improving sensor response efficiency in future. Even though relevant ESIPT phenomenon of DMP-HBT-py molecule could be inferred in experimental manner,[45] as far as we know, experiments could only reveal the indirect information.[31–44] Given current theoretical investigations could provide direct and detailed photo-induced behaviors and excited state dynamical process,[31–44] in this work, we use DFT and TDDFT methods to explore fundamental aspects about different electronic states and interrelated structures. As displayed in Fig. 1, we perform all the full structural optimizations and dynamical simulations using B3LYP/TZVP theoretical level in S_0 and S_1 states using Gaussian 09 software. The specific computational details are shown in Supporting information.

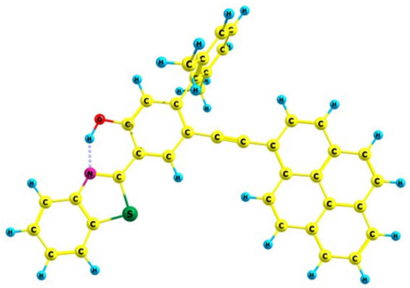

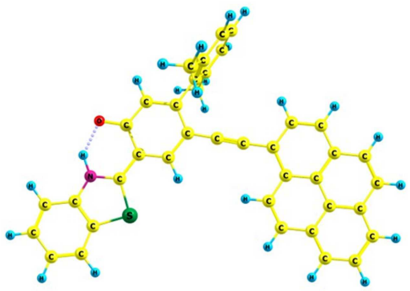

Fig. 1. View of DMP-HBT-py and its proton-transfer DMP-HBT-py-PT tautomer at B3LYP/TZVP (hexane solvent) level. Red: O atom; blue: H atom; yellow: C atom; violet: N atom; green: S atom.

Our paper can be organized as follows: The next section provides results and discussion that describes and discusses our simulated results. It is organized by analyzing formation about hydrogen bonding interactions, changes about geometric structures upon excitation, redistribution of charges in excited state, potential energy curves (PECs), and searching transition state (TS) structure. A final section summarizes and presents the conclusion of the current work.

2. Results and discussion

As is known, atoms-in-molecules (AIM) method is ought to become useful for researching numbers of electrons in AIM basin.[46–48] This technique can also be extended to real space functions like electron localization function (ELF) for small molecules. Given the universality and accuracy of AIM method, herein, we adopt this method to check hydrogen bonding effects for DMP-HBT-py compound. At bond critical point (BCP), we hammer at computing topological parameters of O–H···N for DMP-HBT-py. Via probing into electronic densities $\rho(r)$ and $\nabla^2\rho(r)$, we find $\rho(r)$ of O–H···N is 0.0411 a.u. and $\nabla^2\rho(r)$ is 0.127 a.u. It is quite clear that both $\rho(r)$ and $\nabla^2\rho(r)$ are in the range of hydrogen bonding interactions. Based on molecular electrostatic potential (MEP) for DMP-HBT-py system (shown in Fig. S1 in supporting information), it can be found clearly that the negative electrostatic potential for O atom should be the weakest among all atoms, which reveals the formation of intramolecular hydrogen bond. In addition, in real space, we also compute and show the full weak interactions in DMP-HBT-py compound (see in Fig. S2). The spikes located at -0.02 a.u. ~ -0.01 a.u. appear hydrogen bonding interactions of DMP-HBT-py compound.

For the sake of comparison, the optimized geometrical parameters of O–H···N for DMP-HBT-py are listed in Table 1. Obviously, bond length of O–H of DMP-HBT-py is 0.9924 Å in S_0 state, which changes to become 1.0211 Å in S_1 state. Furthermore, hydrogen bond H···N also changes from S_0-state 1.7378 Å to S_1-state 1.6180 Å. That is to say, upon photoexcitation, hydroxide (O–H) gets longer, which reveals hydrogen bond O–H···N is enhanced.[49–59] The shortening hydrogen bond H···N further indicates O–H···N should be enhanced in S_1 state. Taking the changes of bond angles into consideration, we find δ (O–H–N) of O–H···N is 146.6° in S_0 state, which changes to be 151.1° in S_1 state. Thus, we have reasons to believe that the hydrogen bond O–H···N should be enhanced in S_1 state.[49–59] In addition, for the DMP-HBT-py-PT form, it should be noticed that the S_1-state O···H (1.7569 Å) is shortened to S_0-state (1.5904 Å), while relative H–N is elongated from S_1-state (1.0363 Å) to S_0-state (1.0640 Å). Meanwhile, the bond angle δ (O···H–N) is also enlarged from S1-state (135.6°) to S_0-state (141.0°). That is to say, the much more stable intramolecular hydrogen bond O···H–N is likely to form in the S_0 state via radiation and non-radiation processes from S_1-state DMP-HBT-py-PT form.

Table 1. Optimized geometrical parameters (bond length (in unit Å) and bond angle (in unit (°)) of hydrogen bond O–H···N of DMP-HBT-py and O···H–N of DMP-HBT-py-PT in S_0 and S_1 states based on the DFT/TDDFT methods with IEFPCM (hexane) model.

	DMP-HBT-py		DMP-HBT-py-PT	
	S_0	S_1	S_0	S_1
O–H	0.9924	1.0211	1.5904	1.7569
H–N	1.7378	1.6180	1.0640	1.0363
δ (O–H–N)	146.6°	151.1°	141.0°	135.6°

As far as we know, theoretical simulations about infrared (IR) vibrational spectra should be another effective manner to look into hydrogen bonding interactions.[60–78] To further check the variations of O–H···N between S_0 and S_1 states, we also consider the IR spectral behaviors. As displayed in Fig. 2(a), the IR vibrational peak of O–H stretching mode of DMP-HBT-py compound changes from 3225.39 cm^{-1} (S_0) to 2690.53 cm^{-1} (S_1). That is to say, the enormous redshift 535 cm^{-1} of O–H stretching vibration should be attributed to excited state hydrogen bonding strengthening.[60–78] To sum up, intramolecular hydrogen bond O–H···N of DMP-HBT-py is strengthened, which impetus ESIPT occurrence.

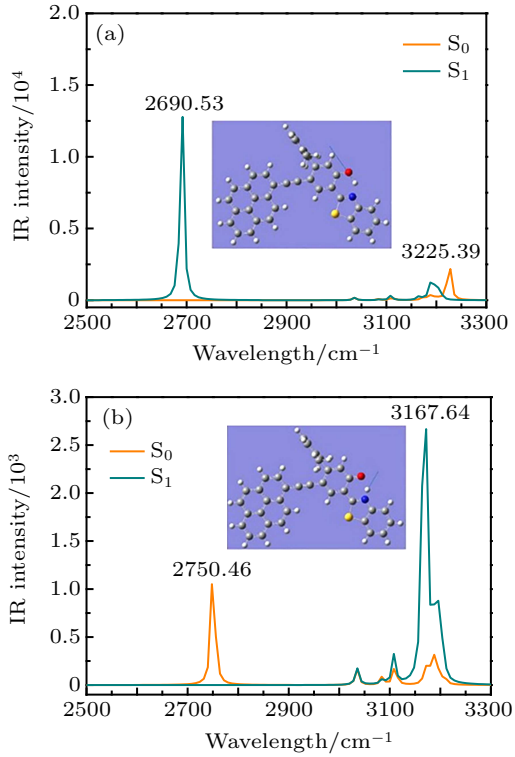

Fig. 2. Simulated IR spectra for DMP-HBT-py (a) and DMP-HBT-py-PT (b) structures in hexane solvent in S_0 and S_1 states. (a) The O–H stretching vibrational mode of DMP-HBT-py form. (b) The H–N stretching vibrational mode of DMP-HBT-py-PT structure.

When it comes to vertical excitation, the reordering of charge densities has a great influence on the dynamics of molecular excited state. As a consequence, we turn our attention to vertical excitation and recombination of electronic densities for DMP-HBT-py compound. The lowest six transitions are calculated in this work. The first two transitions are listed in Table 2, and other transitions are listed in Table S1 in supporting information, Clearly, the first absorption mount of DMP-HBT-py is located at 417 nm consistent with experimental report.[45] Clearly, the first transition $S_0 \rightarrow S_1$ owns the biggest oscillator strength ($f = 0.9397$), which has dominated the entire excitation behaviors. That is to say, the changes of charge caused by $S_0 \rightarrow S_1$ transition could represent the possible dynamical behaviors for DMP-HBT-py compound. According to the above analysis results, the changing behaviors of orbital (*i.e.*, frontier molecular orbitals (MOs)) transitions are further described mainly on $S_0 \rightarrow S_1$ transition. As listed in Table 2, $S_0 \rightarrow S_1$ transition mainly corresponds to the composition from the highest-occupied molecular orbital (HOMO) to the lowest unoccupied molecular orbital (LUMO) with 92.75%, which demonstrates the HOMO → LUMO transition is enough to describe $S_0 \rightarrow S_1$ transition behavior.[49–65] As a result, we only present the HOMO and LUMO in Fig. 3. Obviously, the $S_0 \rightarrow S_1$ should be $\pi\pi^*$-type transition. Concentrating on variations of charge re-organization, the electronic densities around hydroxyl part on HOMO decrease comparing with those on LUMO, while the electronic densities around N atom increase from HOMO to LUMO. Based on theory of valence band, we can say the lone pair electrons of N and σ^* (O–H) orbital impetus ESIPT behavior for DMP-HBT-py compound. In addition, to become more visuals, charge density difference (CDD) map is also shown in Fig. 4 between HOMO and LUMO. It indicates that upon the photoexcitation from S_0 state to S_1 state, net electron densities shift from hydroxyl group to N atom for DMP-HBT-py configuration.

Table 2. Vertical excitation energies (in unit nm), oscillator strengths (f), and relevant transition composition as well as percentage (%) for DMP-HBT-py compound.

	Transition	λ/nm	f	Composition	CI/%
DMP-HBT-py	$S_0 \rightarrow S_1$	417	0.9397	H → L	92.75%
	$S_0 \rightarrow S_2$	336	0.14013	H → L + 1	81.45%
				H-1 → L	8.28%

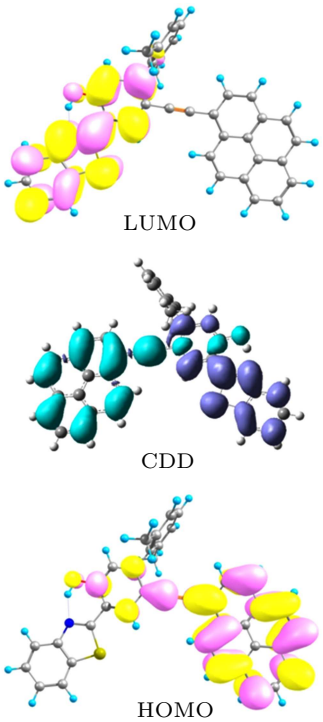

Fig. 3. The HOMO and LUMO of DMP-HBT-py compound via TDDFT/B3LYP/TZVP theoretical level. In CDD map, the regions with increased electron densities are shown in violet, whereas those with decreased electron densities are shown in light blue.

Therefore, it can be predicted that excited-state DMP-HBT-py should favor the deprotonation of hydroxide moiety and the protonation of N group.

Combing hydrogen bonding strengthening with electronic densities re-organization, we can conclude the DMP-HBT-py molecule undergoes the ESIPT reaction. To clarify reaction principle, we further calculate and construct the potential energy curves (PECs) of DMP-HBT-py compound in S_0 and S_1 states. Via restricting O–H bond distance from 0.90 Å to 2.30 Å in step of 0.05 Å, we optimize and show the PECs in Fig. 4(a). In fact, to check the rationality and correctness of B3LYP functional, we also check the PECs using Cam-B3LYP and wB97XD functionals, which present the similar conformation. Therefore, we can confirm the reliability of B3LYP functional. As displayed in Fig. 4, the potential energy increases with the augment of O–H bond in S_0 state, which means the forward PT process is inhibited. However, for S_1-state PEC, a low potential energy barrier (*i.e.*, 1.757 kcal/mol) separates S_1-state DMP-HBT-py and DMP-HBT-py-PT form. Clearly, the low barrier cannot inhibit the ESIPT behavior for DMP-HBT-py system, which facilitates forming proton-transfer tautomer DMP-HBT-py-PT configuration in S_1 state. In fact, in Fig. 2(b), the IR spectra of H–N stretching vibration of DMP-HBT-py-PT form changes from 3167.64 cm^{-1} in S_1 state to 2750.46 cm^{-1} in S_0 state. It indicates the newly formed O···H–N of DMP-HBT-py-PT is stronger in S_0 state. That is, following ESIPT reaction, S_1-state DMP-HBT-py-PT is likely to undergo de-excitation process that proceeds reversed PT with the recovery of initial DMP-HBT-py configuration. Moreover, we also construct the PECs of both S_0 and S_1 states in polar acetonitrile solvent to check whether solvent polarity could affect the ESIPT behavior. The PECs in acetonitrile solvent are shown in Fig. S3 in supporting information. It could be clearly found the potential energy barrier in acetonitrile solvent is very close to toluene solvent. Therefore, we have reasons to believe solvent polarity plays little roles in the ESIPT behavior of DMP-HBT-py system.

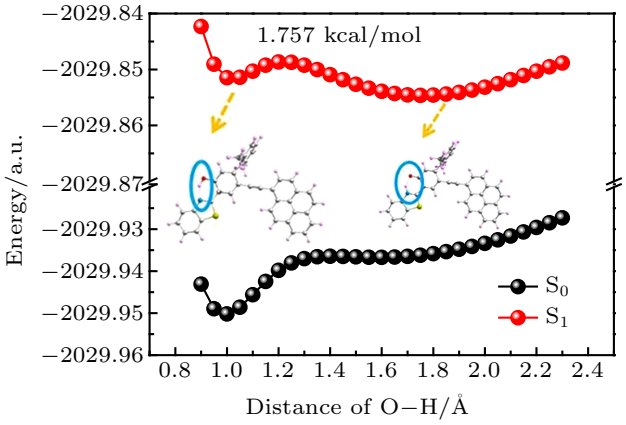

Fig. 4. The constructed PECs of DMP-HBT-py system via fixing O–H bond length in S_0 and S_1 states.

In addition, to check the ESIPT mechanism mentioned above, the calculation of searching transition state (TS) structure is also performed in S_1 state. As displayed in Fig. 5, we simulate and locate the TS form with only one imaginary frequency. Via IR analyses for TS configuration, the vibrational direction of imaginary frequency (−1827.69 cm^{-1}) refers to ESIPT orientation that pushes ESIPT process. Coupling with TS structure, the TS energy barrier for ESIPT is 1.594 kcal/mol, which is consistent with barriers obtained from PECs analyses mentioned above.

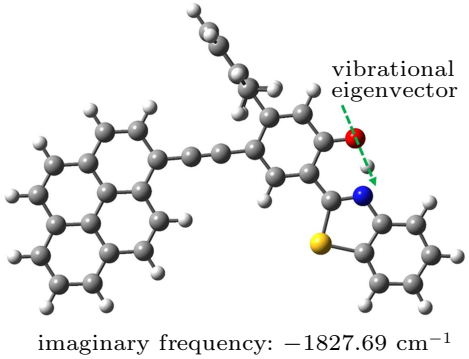

Fig. 5. The TS structure for DMP-HBT-py system along with ESIPT path. Herein, the imaginary frequency and its vibrational eigenvector are also shown.

3. Summary

We mainly concentrate on exploring and elaborating hydrogen bonding interactions and PT mechanism for the novel probe molecule DMP-HBT-py compound. Via exploring the AIM and reduced density gradient *versus* sign(λ_2)ρ of DMP-HBT-py, we verify the formation and stabilization of intramolecular hydrogen bond O–H···N in S_0 state. Insights into the structural modifications (*i.e.*, bond distance and bond angle) and IR spectra for DMP-HBT-py compound, the strengthening phenomena of O–H···N for DMP-HBT-py compound could be validated in perspective. Combing with the analyses of photo-induced electronic densities recombination, we prove the hydrogen bonding strengthening and charge organization could provide the driving force for promoting ESIPT process. Meanwhile in Switzerland, exploring the potential barrier in different functionals, we present the ultrafast ESIPT mechanism for DMP-HBT-py. Coupling with TS form analyses, furthermore, we amply confirm the ultrafast behavior for DMP-HBT-py compound. We sincerely hope that our theoretical work could provide novel insights and promote efficient solid emitters in OLEDs in future.

References

[1] Zhao G and Han K 2012 *Acc. Chem. Res.* **45** 404
[2] Zhao G, Han K, Lei Y and Dou Y 2007 *J. Chem. Phys.* **127** 094307
[3] Li J, Wu Y, Xu Z, Liao Q, Zhang H, Zhang Y, Xiao L, Yao J and Fu H 2017 *J. Mater. Chem. C* **5** 12235
[4] Zhao J, Dong H, Yang H and Zheng Y 2018 *Org. Chem. Front* **5** 2710
[5] Zhao H, Sun C, Liu X, Yin H and Shi Y 2019 *Chin. Phys. B* **28** 018201

[6] Zhao J, Dong H and Zheng Y 2018 *J. Lumin.* **195** 228
[7] Miao C and Shi Y 2011 *J. Comput. Chem.* **32** 3058
[8] Demchenko A, Tang K and Chou P 2013 *Chem. Soc. Rev.* **42** 1379
[9] Zhao J, Chen J, Liu J and Hoffmann M 2015 *Phys. Chem. Chem. Phys.* **17** 11990
[10] Qu R, Liu H, Feng M, Yang X and Wang Z 2012 *J. Chem. Eng. Data* **57** 2442
[11] Li G and Chu T 2011 *Phys. Chem. Chem. Phys.* **13** 20766
[12] Liu S, Pan J, Wei D, Xu J, Zhou Y and Song Y 2019 *Can. J. Phys.* **97** 721
[13] Zhang M, Zhou Q, Du C, Ding Y and Song P 2016 *RSC Adv.* **6** 59389
[14] Yin H and Shi Y 2018 *Chin. Phys. B* **27** 058201
[15] Zhao J, Dong H and Zheng Y 2018 *J. Phys. Chem. A* **122** 1200
[16] Li G, Li W, Zhang H and Sun X 2014 *J. Theor. Comput. Chem.* **13** 1450006
[17] Li G, Wang J, Zhang H, Li W, Wang F and Liang Y 2014 *Chem. Phys. Lett.* **616** 30
[18] Ma H and Huang J 2016 *RSC Adv.* **6** 96147
[19] Zhao J, Chen J, Cui Y, Wang J, Xia L, Dai Y, Song P and Ma F 2015 *Phys. Chem. Chem. Phys.* **17** 1142
[20] Li H, Ma L, Yin H and Shi Y 2018 *Chin. Phys. B* **27** 098201
[21] Liu S, Ma Y, Yang Y, Liu S, Li Q and Song Y 2018 *Chin. Phys. B* **27** 023103
[22] Chen H, Zhao J, Huang J and Liang Y 2019 *Phys. Chem. Chem. Phys.* **21** 7447
[23] Zhao J and Zheng Y 2017 *Sci. Rep.* **7** 44897
[24] Xiao H, Chen, K, Cui D, Jiang N, Yin G, Wang J and Wang R 2014 *New J. Chem.* **38** 2386
[25] Stasyuk A, Chen Y, Chen C, Wu P and Chou P 2016 *Phys. Chem. Chem. Phys.* **18** 24428
[26] Tang K, Chen C, Chuang H, Chen J, Chen Y, Lin Y, Shen J, Hu W and Chou P 2011 *J. Phys. Chem. Lett.* **2** 3063
[27] Dahal D, McDonald L, Bi X, Abeywickrama C, Gombedza F, Konopka M, Paruchuri S and Pang Y 2017 *Chem. Commun.* **53** 3697
[28] Wang J, Li Y, Duah E, Paruchuri S, Zhou D and Pang Y 2014 *J. Mater. Chem. B* **2** 2008
[29] Zhang X, Han J, Li Y, Sun C, Su X, Shi Y and Yin H 2020 *Chin. Phys. B* **29** 038201
[30] Liu X, Yin H, Li H and Shi Y 2017 *Spectrochim. Acta Part. A* **177** 1
[31] Zhao J, Liu X and Zheng Y 2017 *J. Phys. Chem. A* **121** 4002
[32] Li H, Yin H, Liu X, Shi Y, Jin M and Ding D 2017 *Spectrochim. Acta Part. A* **184** 270
[33] Xu L, Zhang T, Zhang Q and Yang D 2020 *Chin. Phys. B* **29** 053102
[34] Zhao J, Chen J, Song P, Liu J and Ma F 2015 *J. Clust. Sci.* **26** 1463
[35] Wan M, Jin C, Yu Y, Huang D and shao J 2017 *Chin. Phys. B* **26** 033101
[36] Zhao J and Yang Y 2016 *J. Mol. Liq* **220** 735
[37] Li W, Guo B, Chang C, Guo X, Zhang M and Li Y 2016 *J. Mater. Chem. A* **4** 10135
[38] Li X, Zhai Y, Zhang M and Song Y 2018 *J. Phys. Org. Chem.* **31** 3821
[39] Zhao J, Song P and Ma F 2014 *Commun. Comput. Chem.* **2** 117
[40] Peng C, Shen J, Chen Y, Wu P, Hung W, Hu W and Chou P 2015 *J. Am. Chem. Soc.* **137** 14349
[41] Abeywickrama C, Wijesinghe K, Stahelin R and Pang Y 2017 *Chem. Commun.* **53** 5886
[42] Zhao J, Dong H, Yang H and Zheng Y 2019 *ACS Appl. Bio. Mater.* **2** 5182
[43] Kumar G, Paul K and Luxami V 2020 *New J. Chem.* **44** 12866
[44] Nguyen H, Trinh B, Nguyen N, Dang S, Phama H and Dguyen L 2011 *Phytochem. Lett.* **4** 48
[45] Niu Y, Wang R, Pu L and Zhang Y 2019 *Dyes Pigm.* **170** 107594
[46] Bultinck P, Alsenoy C, Ayers P and Carbo-Dorca R 2007 *J. Chem. Phys.* **126** 144111
[47] Geldof D, Krishtal A, Blockhuys F and Alsenoy C 2011 *J. Chem. Theory Comput.* **7** 1328
[48] Verstraelen T, Ayers P, Speybroeck V and Waroquier M 2013 *J. Chem. Theory Comput.* **9** 2221
[49] Zhao J, Yao H, Liu J and Hoffmann M 2015 *J. Phys. Chem. A* **119** 681
[50] Zhou L, Liu J, Zhao G, Shi Y, Peng X and Han K 2007 *Chem. Phys.* **333** 179
[51] Rocard J, Berezin A, Leo F and Bonifazi D 2015 *Angew. Chem. Int. Ed.* **54** 15739
[52] Zhao J and Li P 2015 *RSC Adv.* **5** 73619
[53] Moorthy J, Natarajan P, Venkatakrishnan, Huang D and Chow T 2007 *Org. Lett.* **9** 5215
[54] Zhao G, Northrop B, Stang P and Han K 2010 *J. Phys. Chem. A* **114** 3418
[55] Garo F and Haner R 2012 *Angew. Chem. Int. Ed.* **51** 916
[56] Nakazato T, Kamatsuka T, Inoue J, Sakurai T, Seki S, Shinokubo H and Miyake Y 2018 *Chem. Commun.* **54** 5177
[57] Wang Y, Jia M, Zhang Q, Song X and Yang D 2019 *Chin. Phys. B* **28** 103105
[58] Zhao G, Northrop B, Han K and Stang P 2010 *J. Phys. Chem. A* **114** 9007
[59] Zhao G, Chen R, Sun M, Liu J, Li G, Gao Y, Han K, Yang X and Sun L 2008 *Chem. Eur. J.* **14** 6935
[60] Yin H, Zhang Y, Zhao H, Yang G, Shi Y, Zhang S and Ding D 2018 *Dyes Pigm.* **159** 506
[61] Han J, Liu X, Sun C, Li Y, Yin H and Shi Y 2018 *RSC Adv.* **8** 29589
[62] Li H, Han J, Zhao H, Liu X, Luo Y, Shi Y, Liu C, Jin M and Ding D 2019 *J. Phys. Chem. Lett.* **10** 748
[63] Fan G, Han K and He G 2013 *Chin. J. Chem. Phys.* **26** 635
[64] Cong L, Yin H, Shi Y, Jin M and Ding D 2015 *RSC Adv.* **5** 1205
[65] Li H, Han J, Zhao H, Liu X, Ma L, Sun C, Yin H and Shi Y 2018 *J. Clust. Sci.* **29** 585
[66] Merrick J, Moran D and Radom L 2007 *J. Phys. Chem. A* **111** 11683
[67] Palafox M, Talaya J, Guerrero-Martinez A, Tardajos G, Kumar H, Vats J and Rastogi V 2010 *Spectrosc. Lett.* **43** 51
[68] Zhao J, Dong H, Yang H and Zheng Y 2019 *ACS Appl. Bio. Mater* **2** 2060
[69] Zhang M, Zhou Q, Zhang M, Dai Y, Song P and Jiang Y 2017 *J. Clust. Sci.* **28** 1191
[70] Qu R, Zhang Q, Zhang X and Wang Z 2012 *Spectrosc. Lett.* **45** 240
[71] Tang K, Chang M, Lin T, Pan H, Fang T, Chen K, Hung W, Hsu Y and Chou P 2011 *J. Am. Chem. Soc.* **133** 17738
[72] Chou P, Wei C, Wu G and Chen W 1999 *J. Am. Chem. Soc.* **121** 12186
[73] Hsieh C, Chou P, Shih C, Chuang W, Chung M, Lee J and Joo T 2011 *J. Am. Chem. Soc.* **133** 2932
[74] Tseng H, Liu J, Chen Y, Chao C, Liu K, Chen C, Lin T, Hung C, Chou Y, Lin T, Wang T and Chou O 2015 *J. Phys. Chem. Lett.* **6** 1477
[75] Wang J, Chu Q, Liu X, Wesdemiotis C and Pang Y 2013 *J. Phys. Chem. B* **117** 4127
[76] Wang J, Liu X and Pang Y 2014 *J. Mater. Chem. B* **2** 6634
[77] McDonald L, Liu B, Taraboletti A, Whiddon K, Shriver L, Konopka M, Liu Q and Pang Y 2016 *J. Mater. Chem. B* **4** 7902
[78] Wang J, Chen W, Liu X, Wesdemiotis C and Pang Y 2014 *J. Mater. Chem. B* **2** 3349